TISSUE ENGINEERING: Part A
Volume 17, Numbers 9 and 10, 2011

DOI: 10.1089/ten.tea.2010.0535

Dynamic Tensile Loading Improves the Functional Properties of Mesenchymal Stem Cell-Laden Nanofiber-Based Fibrocartilage

Brendon M. Baker, Ph.D.,[1,2] Roshan P. Shah, M.D., J.D.,[1] Alice H. Huang, Ph.D.,[1,2] and Robert L. Mauck, Ph.D.[1,2]

Fibrocartilaginous tissues such as the meniscus serve critical load-bearing roles, relying on arrays of collagen fibers to resist tensile loads experienced with normal activity. As these structures are frequently injured and possess limited healing capacity, there exists great demand for tissue-engineered replacements. Toward re-creating the structural features of these anisotropic tissues *in vitro*, we employ scaffolds composed of co-aligned nanofibers that direct mesenchymal stem cell (MSC) orientation and the formation of organized extracellular matrix (ECM). Concomitant with ECM synthesis, the mechanical properties of constructs increase with free-swelling culture, but ultimately failed to achieve equivalence with meniscal fibrocartilage. As mechanical forces are essential to the development and maintenance of musculoskeletal tissues, this work examined the effect of cyclic tensile loading on MSC-laden nanofibrous constructs. We hypothesized that loading would modulate the transcriptional behavior of MSCs, spur the deposition of ECM, and lead to enhancements in construct mechanical properties compared to free-swelling controls. Fiber-aligned scaffolds were seeded with MSCs and dynamically loaded daily in tension or maintained as nonloaded controls for 4 weeks. With mechanical stimulation, fibrous gene expression increased, collagen deposition increased, and the tensile modulus increased by 16% relative to controls. These results show that dynamic tensile loading enhances the maturation of MSC-laden aligned nanofibrous constructs, suggesting that recapitulation of the structural and mechanical environment of load-bearing tissues results in increases in functional properties that can be exploited for tissue engineering applications.

Introduction

The meniscus is a dense fibrocartilaginous tissue that plays a crucial role in normal knee function.[1,2] These semilunar wedges, situated between the femoral condyles and tibial plateau, function to transfer and absorb loads by redirecting vertical forces laterally, efficiently converting compressive into tensile loads via a hoop-stress mechanism.[3] These forces are borne by a highly organized extracellular matrix (ECM) composed of circumferentially oriented collagen bundles that form the bulk of the tissue and instill mechanical anisotropy, a characteristic vital to the function of the tissue.[4–6] Compositionally, collagens make up 85%–95% of the tissue,[7,8] whereas proteoglycans, comprising 2%–3% of the dry weight, are concentrated in the more cartilage-like inner region and contribute to the compressive properties of the tissue.[9,10] With normal physiologic loading, forces several times body weight arise within the knee.[11,12] Given the high tensile stiffness in the circumferential direction (65–80 MPa),[13] the menisci transmit 50%–100% of these forces with strains of only to 2%–6%.[14,15]

While the meniscus functions well with normal use, damage may occur as a result of traumatic events and/or age-related degenerative processes.[16,17] Meniscal damage frequently manifests in the form of tears that disrupt the circumferentially aligned collagen fiber architecture, thereby abrogating normal mechanical function, increasing stresses on the adjacent articular surfaces, and initiating osteoarthritic sequelae in the joint.[2,18] The current standard of treatment for such tears is resection of the damaged portion of the tissue through partial or total meniscectomy, a procedure that fails to restore normal mechanics in the knee and predisposes the patient to precocious osteoarthritic changes.[19,20] Thus, there exists considerable clinical demand for a repair strategy that restores meniscal function and protects against further deleterious changes in the joint.

With the eventual goal of replacing damaged meniscus with engineered fibrocartilage that has structural, mechanical, and biochemical features similar to the healthy native tissue, we have employed aligned nanofibrous scaffolds.[21] These scaffolds are formed by the electrospinning process, wherein a polymer solution is drawn into fiber form through

[1]McKay Orthopaedic Research Laboratory, Department of Orthopaedic Surgery, and [2]Department of Bioengineering, University of Pennsylvania, Philadelphia, Pennsylvania.

a voltage gradient and collected layer by layer on a grounded surface.[22] With focused deposition onto a rotating mandrel, this simple electrostatic process produces three-dimensional scaffolds composed of aligned polymer fibers with tunable mechanical and structural anisotropy.[23–25] Beyond mimicking the microstructural features and length scales of natural collagenous ECMs, aligned nanofibrous scaffolds recapitulate the mechanical behavior and structural organization of anisotropic fiber-reinforced soft tissues such as the meniscus.[26] Most importantly, these scaffolds serve as an instructive three-dimensional micropattern for directed cell-mediated collagen-rich ECM deposition. On poly(ε-caprolactone) nanofibrous scaffolds, numerous cell types will align, deposit ordered collagen, and increase construct tensile properties in the direction of nanofiber alignment.[21] Conversely, when seeded on randomly oriented nanofibers, cellular orientation and matrix deposition is disorganized and so the resulting changes in mechanical properties are marginal.

Mesenchymal stem cells (MSCs) are a cell type especially amenable to instruction from a nanofibrous microenvironment. MSCs are a self-renewing population of multipotent cells under widespread investigation for applications in regenerative medicine,[27,28] and in particular, we have explored their utility as a cell source for engineering fibrocartilaginous tissues such as the knee meniscus and the annulus fibrosus of the intervertebral disc.[21,29] These cells may be directed along numerous tissue-specific lineages by modulation of their chemical, mechanical, and topographical environment.[30,31] On nanofibrous scaffolds in the presence of transforming growth factor-beta 3 (TGF-β3), MSCs adopt an elongated morphology and express fibrous over chondrogenic markers in a chemical environment permissive to both phenotypes.[32] Previous studies conducted in static, free-swelling conditions showed that MSCs synthesize organized fibrocartilaginous ECM on aligned nanofibrous scaffolds, leading to increases in the tensile modulus of cell–scaffold constructs.[21] However, even with long-term culture (100 days), endpoint tensile properties reached a maximum of 30 MPa, a value below native meniscus tissue by two-fold or more.[33] While results from these studies indicate MSCs in conjunction with aligned nanofibrous scaffolds hold promise for engineering anisotropic fibrocartilage, free-swelling culture does not provide sufficient stimuli to drive tissue formation toward functional equivalence with the native meniscus.

Load transmission is not only the chief function of musculoskeletal tissues, but also a driving force vital to their development and homeostatic maintenance.[34] For instance, the absence of forces in avian hind limbs inhibited the normal patterning and formation of tendons.[35] In forming synovial joints, contracting peripheral musculature plays a fundamental role in progenitor cell fate commitment and subsequent joint cavitation and morphogenesis.[36] In specific regard to the meniscus, while the early stages of meniscal formation proceed normally in the developing knees of immobilized chick embryos, these tissues ultimately fail to mature and are eventually resorbed in the absence of load transmission.[37] Based on these observations, there has been much interest in recapitulating physiologic forces *in vitro* toward spurring the development of engineered musculoskeletal tissues.[38] Cyclic compression of cartilage constructs enhances mechanical and biochemical outcomes[39] and repeated tensile loading promotes matrix gene expression, deposition, and tissue maturation for tendon and ligament applications.[40,41] Notably, Lee and coworkers performed short-term stretching (3 days) of ligament fibroblasts on thin layers of aligned nanofibers, detecting an increase in collagen production with loading that was sensitive to cellular orientation.[42] Toward enhancing the formation of MSC-based tissues, reports indicate that cyclic compression of hydrogel constructs reinforces MSC chondrogenesis,[43–45] and cyclic tension of fibrin gels upregulates fibrous gene expression.[46] Taken together, these studies demonstrate that dynamic loading representative of physiologic loading can drive MSC differentiation, modulate biosynthetic activity, and lead to the production of engineered replacement tissues that better approximate their native counterparts.

Based on these findings, the current study explored the effects of dynamic tensile loading on MSC-seeded aligned nanofibrous scaffolds. After establishing a fibrochondrogenic population of aligned MSCs, we hypothesized that tensile stimulation would upregulate fibrous markers representative of fibrocartilage, increase the production of collagenous ECM, and, as a result, improve the functional properties of constructs. Toward this end, a bioreactor system was designed and validated for dynamic loading of nanofibrous constructs during *in vitro* culture. The effects of cyclic tension on the long-term maturation of MSC-seeded aligned nanofibrous scaffolds were examined, with transcriptional, biochemical, and mechanical changes examined over 4 weeks of cyclic loading.

Materials and Methods

Scaffold fabrication

For bioreactor validation and cell-seeded studies, separate, aligned, nanofibrous meshes were produced via electrospinning as described previously.[21] Briefly, a 14.3% w/v solution of poly(ε-caprolactone) (80 kDa; Sigma-Aldrich, St. Louis, MO) was dissolved in a 1:1 solution of tetrahydrofuran and *N*,*N*-dimethylformamide (Fisher Chemical, Fairlawn, NJ). This solution was supplied to the spinneret tip at a rate of 2 mL/h via syringe pump (KDS100; KD Scientific, Holliston, MA). A power supply (ES30N-5W; Gamma High Voltage Research, Ormond Beach, FL) was used to apply a +10 kV potential difference between the spinneret and the aluminum mandrel (Ø = 2″). Aluminum shields were charged to +5 kV to aid in directing the transiting electrospun fibers toward the mandrel, which was charged to −3 kV. To induce fiber alignment, the mandrel was rotated via a belt mechanism conjoined to an AC motor (Pacesetter 34R; Bodine Electric, Chicago, IL) to achieve a linear surface velocity of ~10 m/s. Nanofibers were collected over a spinneret-mandrel distance of 15 cm for 4 h, resulting in mats of ~600 μm thickness.

Cyclic tension bioreactor

A custom bioreactor was designed and constructed for applying cyclic sinusoidal deformations to cell-seeded nanofibrous scaffolds during *in vitro* culture (Fig. 1). The device is founded on a stepper motor linked to a bi-directional lead screw, which drives the opposing motion of two sliding carriages (BiSlide; Velmex, Bloomfield, NY). Before tensile

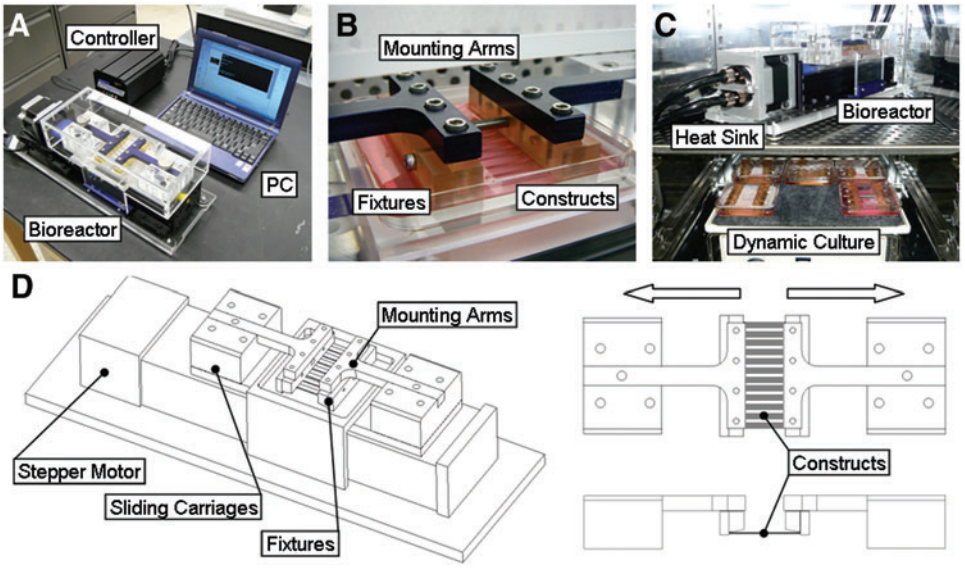

FIG. 1. Tensile bioreactor design. **(A)** The device consists of a computer programmable stepper motor that drives the opposing motion of two linear stages. **(B)** These stages are linked to mounting arms designed to engage and distract fixtures containing multiple cell-seeded scaffolds. **(C)** A heat sink is placed on the motor to remove excess heat during operation in a standard incubator. When not loaded, samples are cultured dynamically on an orbital shaker to ensure even nutrient distribution to arrays of clamped constructs. **(D)** Schematics of the tensile bioreactor and fixture assembly. Color images available online at www.liebertonline.com/tea

loading, samples were mounted and cultured in custom polysulfone fixtures (Fig. 1). These autoclavable and chemically inert sample grips engaged the sliding carriages via anodized aluminum mounting arms, and additionally served to maintain the positioning of samples during rest periods. This modular design enables ready insertion, loading, and removal of sets of samples, allowing multiple experimental groups to be loaded daily. To maintain sterility, the entire assembly was covered by an acrylic lid, which also provided a means for sample observation during loading. Heat generated by the stepper motor was removed from the incubator via a coolant-circulating heat sink (Koolance, Auburn, WA). Motion of the stepper motor was defined via control software (COSMOS; Velmex) to execute a variety of waveforms with a resolution of 6.4 μm (defined by a single step of the motor). The maximum carriage velocity was 38 mm/s and sample lengths were maintained at 48 mm, translating to a maximum strain rate of 160%/s given the linked and opposite translations of the two carriages. In this work, the device was programmed to approximate sinusoidal waveforms equating to 3% strain amplitude (0%–6% strain) at a frequency of 1 Hz.

Bioreactor validation and fatigue testing

Before dynamically loading cell-seeded scaffolds, programmed carriage motions were confirmed to translate to accurate and repeatable deformations of nanofibrous scaffolds. Acellular scaffolds (5×60 mm) were airbrushed with black enamel to generate surface texture and placed within the bioreactor. Loading was initiated, and images of the central 50% width of each specimen were captured for subsequent texture-correlation analysis via Vic2D to determine two-dimensional Lagrangian strain (Correlation Solutions, Columbia, SC). With an applied deformation to sub-yield strains, aligned nanofibrous scaffolds develop nonrecoverable slack causing the sample to move out of the plane of focus. Therefore, samples were prestrained to 1%, and then cyclically loaded an additional 5% up to 1000 cycles. In additional studies, acellular scaffolds were loaded to 6% strain for either 108,000 or 216,000 cycles in PBS, a number of cycles equivalent to that experienced by cell-seeded constructs.

Cell isolation, expansion, and seeding

MSCs were isolated from tibial and femoral bone marrow of two 3–6-month-old calves (Research 87, Boylston, MA) as described in Ref. 47. Briefly, marrow was freed from the trabecular spaces via agitation in Dulbecco's modified Eagle's medium (DMEM) supplemented with 300 units/mL heparin. After centrifugation for 5 min at 500 *g*, the pelleted matter was resuspended in DMEM containing 1× penicillin/streptomycin/Fungizone and 10% fetal bovine serum and plated in 150 mm tissue culture dishes. Adherent cells formed numerous colonies through the first week, and were subsequently expanded through passage 2 at a ratio of 1:3.

Scaffolds (60×5 mm, with the long axis oriented in the direction of nanofiber alignment) were sterilized and rehydrated in decreasing concentrations of ethanol (100%, 70%, 50%, and 30%; 30 min/step), concluding with two washes in PBS. A 100 μL aliquot containing 1×10^6 MSCs was loaded onto each side of the scaffold followed by 1 h of incubation to allow for cell attachment. After seeding, cell–scaffold constructs were cultured individually in custom troughs (to accommodate the large sample length) for 6 weeks in chemically defined medium (high-glucose DMEM with 1× penicillin/streptomycin/Fungizone, 0.1 μM dexamethasone, 50 μg/mL ascorbate 2-phosphate, 40 μg/mL L-proline, 100 μg/mL sodium pyruvate, 6.25 μg/mL insulin, 6.25 μg/mL transferrin, 6.25 ng/mL selenious acid, 1.25 mg/mL bovine serum albumin, and 5.35 μg/mL linoleic acid containing 10 ng/mL TGF-β3).

Tensile loading

After this initial 6-week preculture period, constructs were transferred to fixtures for long-term dynamic mechanical stimulation. Each day, constructs were mounted into the bioreactor and cyclically loaded to 6% strain at a frequency of 1 Hz for 3 h. During rest periods, construct assemblies were placed on an orbital shaker to ensure even nutrient

distribution to all samples. To serve as nonloaded controls, an additional set of constructs were clamped in identical fixtures and maintained for the duration of the study on the orbital shaker. Medium changes occurred every 2 days.

Mechanical testing

Acellular scaffolds from fatigue loading and cell-seeded constructs were mechanically tested through uniaxial extension to failure to determine tensile properties. Before testing, cross-sectional area was determined at four locations along the length of each sample with a custom laser-LVDT measurement system.[48] Testing was performed with an Instron 5848 Microtester (Instron, Canton, MA). After a 0.1N preload for 60 s to remove slack, gauge length was noted, and samples were extended to failure at a rate of 0.1% of the gauge length per second. Stiffness was determined over a 1% strain range from the linear region of the force–elongation curve with a custom MATLAB script. Using the cross-sectional area and gauge length, Young's modulus was calculated from the analogous stress–strain curve. Gauge lengths were maintained across groups and time points, to enable the comparison of stiffness among samples.

Biochemical and gene expression analyses

After mechanical testing, samples were stored at $-20°C$ until processing to determine biochemical composition. Samples were digested in papain as in Ref. 47 and assayed for DNA, sulfated glycosaminoglycan (GAG), and collagen content using the Picogreen double-stranded DNA (Molecular Probes, Eugene, OR), DMMB dye-binding,[49] and orthohydroxyproline[50] assays, respectively. Hydroxyproline content was converted to collagen as in Ref. 51, using a factor of 7.14.

An additional portion of each construct was finely minced and homogenized in TRIZOL (Invitrogen, Carlsbad, CA). Total RNA was extracted in phenol/chloroform and reverse transcribed as in Ref. 52. Real-time polymerase chain reaction was carried out with intron-spanning primers for type I and II collagen, fibronectin, lysyl oxidase, and glyceraldehyde 3-phosphate dehydrogenase (GAPDH). Starting quantities of target transcripts were determined by the standard curve method and normalized to GAPDH levels determined similarly.

Statistical analysis

Analysis of variance (ANOVA) was carried out with SYSTAT (v10.2, Point, Richmond, CA), with Bonferroni *post hoc* tests used to make pair-wise comparisons between groups when necessary. Significance was set at $p \leq 0.05$. For acellular scaffold studies, a one-way ANOVA was performed with the factor of loading duration. To test significance in biochemical and mechanical data of cell-seeded studies, two-way ANOVAs were performed with culture duration and application of loading as independent factors. Gene expression results were tested with a one-way ANOVA with application of loading as the single factor. To assess agreement between programmed bioreactor deformations and resulting strains, Bland-Altman limits of agreement (bias ± standard deviation) were computed. All data are presented as the mean ± the standard deviation.

Results

Bioreactor validation and fatigue loading

To confirm that strains applied by the bioreactor were accurate and reproducible, texture correlation was used to determine two-dimensional strains of acellular scaffolds during loading. Average surface strains approximated a sinusoidal waveform and consistently achieved the target strain of 6% over 1000 cycles (Fig. 2A). When comparing theoretical and applied strains over the thousandth cycle, the Bland-Altman limits of agreement were -0.004 ± 0.003 strain. Surface strains across the central 50% width of each scaffold were homogeneous at the peak and trough of both initial and late loading cycles, where the standard deviation in strain across the area of interest was < 0.005 across all cycles analyzed (Fig. 2B).

To examine the effect of repeated deformations on scaffold mechanical properties, acellular scaffolds were cyclically loaded for either 108,000 or 216,000 cycles, equivalent to the number of loading events encountered by cell-seeded constructs with loading at 1 Hz for 3 h per day over a 2- or 4-week period. After 108,000 cycles, the tensile stress response of scaffolds decreased slightly, particularly at higher strains (5%–10% region, Fig. 2C), with this translating to an 11% decrease in tensile modulus ($p < 0.01$, Fig. 2D). Normalizing to the stiffness of nonloaded controls, the equivalent of 2 weeks of loading led to a 6% decrease in stiffness ($p < 0.01$, Fig. 2E). An additional 108,000 cycles did not elicit further changes in the stress–strain response ($p = 1.0$), suggesting that after these initial decreases, additional loading did not further compromise acellular scaffold mechanical properties.

Construct preculture and effect of dynamic culture conditions

Fiber-aligned nanofibrous scaffolds were seeded with MSCs and precultured for a period of 6 weeks, after which samples were either loaded daily for an additional 2 or 4 weeks or maintained as nonloaded controls (Fig. 3). During the preculture period, constructs were cultured individually under static conditions where the media remained unperturbed. Under these conditions, MSCs colonized scaffolds and simultaneously elaborated a functional fibrocartilaginous matrix, consistent with previous studies.[21] The production of collagen and proteoglycans, key matrix constituents of fibrocartilage, was evident from biochemical assays (Fig. 4B, C) and by histologic staining (Fig. 5).

After the initial 6-week preculture period, all remaining constructs were placed in fixtures designed to interface with the bioreactor and cultured upon an orbital shaker to ensure even nutrient distribution across samples. With 2 weeks of culture under dynamic media conditions, a marked loss in proteoglycan content of both loaded and nonloaded constructs was evident, with nearly a 50% reduction in GAG content (Fig. 4C). After this initial decline, nonloaded controls continued to lose proteoglycans ($p < 0.001$ vs. week 8), whereas loaded constructs reached a steady state ($p = 1.0$ vs. week 8). This proteoglycan loss was readily apparent when comparing cross sections of precultured and week 10 constructs stained for proteoglycans (Fig. 5). Dynamic culture did not adversely impact collagen content, as both loaded

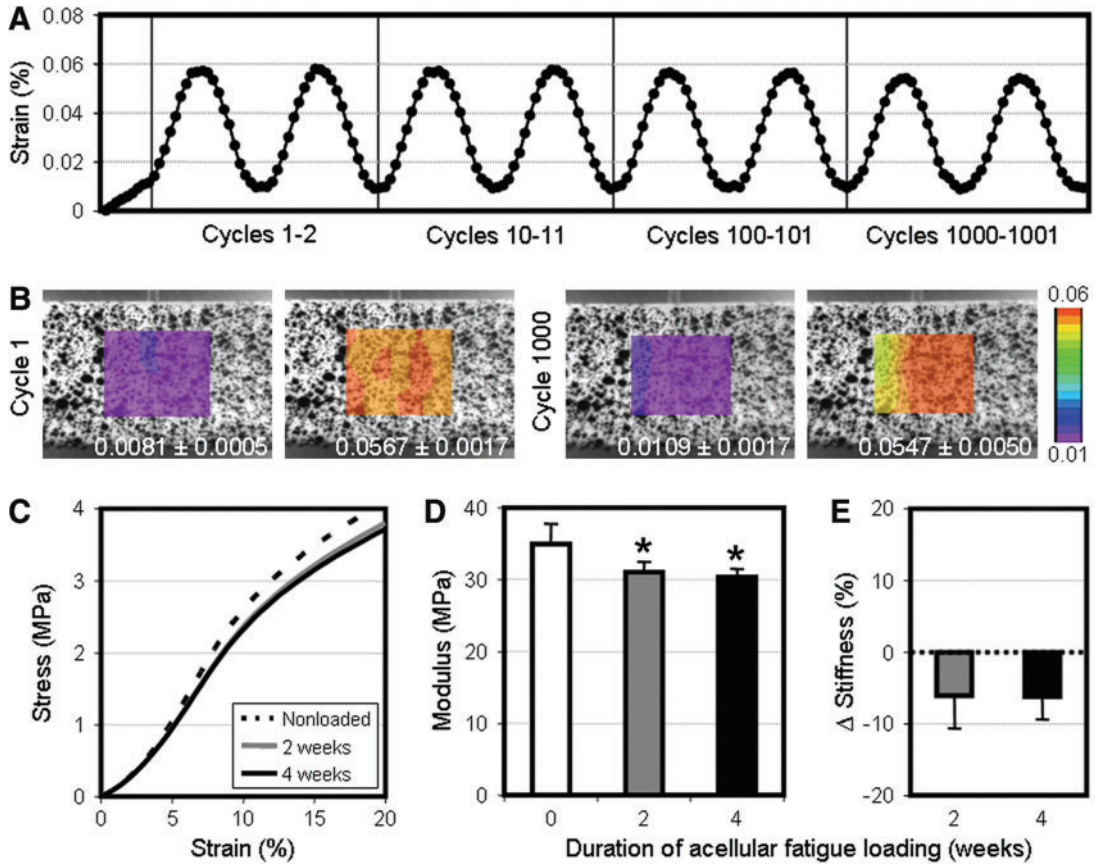

FIG. 2. Bioreactor validation and fatigue testing of acellular scaffolds. **(A)** Average surface strains determined by texture correlation of acellular scaffolds preloaded to 1% strain and cyclically loaded to 6% strain at 0.1 Hz. **(B)** Representative strain maps of speckled scaffolds at minimum and maximum deformation during cycle 1 and 1000. Values within each image denote the average ± standard deviation strain values taken across each region of analysis. Average stress–strain curves **(C)**, tensile modulus **(D)**, and percentage change in stiffness (normalized to nonloaded scaffolds) **(E)** after 2 weeks (108,000 cycles) or 4 weeks (216,000 cycles) of loading to 6% strain at 1 Hz ($n=6$, $^*p<0.05$ vs. nonloaded samples). Color images available online at www.liebertonline.com/tea

and nonloaded constructs continued to accrue collagen after the preculture period (Fig. 4B).

Effect of dynamic loading on construct maturation

Dynamically loaded and nonloaded control constructs were analyzed for biochemical content at weeks 8 and 10.

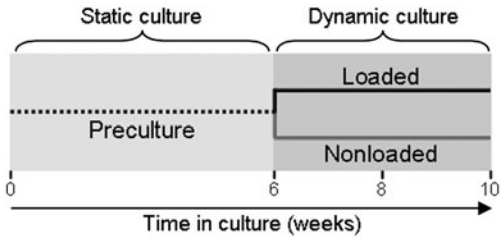

FIG. 3. Study design. Aligned nanofibrous scaffolds were seeded with mesenchymal stem cells (MSCs) and precultured for an initial 6-week period under static culture conditions. After this, samples were either loaded daily or maintained as nonloaded controls for up to an additional 4 weeks. Constructs were harvested at weeks 6, 8, and 10 for analysis.

Over the first 2 weeks of cyclic conditioning, there was a significant decrease in DNA content in loaded constructs compared to both preculture samples and nonloaded controls ($p<0.001$, Fig. 4A). DNA content did not decrease further with an additional 2 weeks of loading ($p=0.62$). Despite a decrease in cellularity due to loading, cells continued to secrete collagenous matrix. At week 8, both loaded and nonloaded constructs increased in collagen content relative to preculture values, with no difference between groups at this time point ($p=1.0$, Fig. 4B). However, while the collagen content of nonloaded controls plateaued by week 10 ($p=1.0$ vs. week 8), mechanically conditioned constructs continued to accrue collagen ($p<0.001$ vs. week 8). At the terminal time point, dynamically loaded constructs contained more collagen than nonloaded controls ($p<0.005$). Construct cross sections stained for collagen revealed slightly more intense staining in loaded constructs as compared to nonloaded controls (Fig. 5). No differences in proteoglycan content were observed with mechanical loading ($p>0.79$, Fig. 4C), consistent with Alcian blue staining (Fig. 5).

Mechanical properties of constructs at the beginning and end of the preculture period, and loaded samples and nonloaded counterparts at weeks 8 and 10 were evaluated in tension. Overall, increases in construct tensile properties

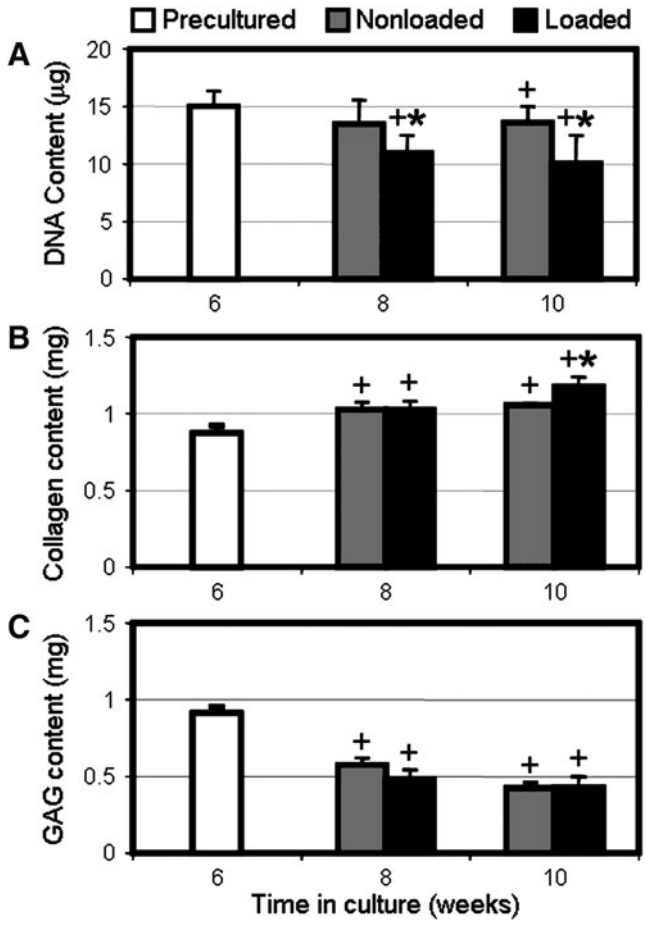

FIG. 4. Effect of dynamic culture and tensile loading on biochemical content. Total DNA **(A)**, collagen **(B)**, and glycosaminoglycan (GAG) **(C)** content of MSC-seeded constructs after preculture (week 6), and with up to 4 weeks of daily cyclic loading ($n=6$, $^*p<0.05$ vs. nonloaded controls, $+p<0.05$ vs. precultured constructs).

were reflective of changes in collagen content. As constructs accumulated collagen throughout the preculture period, the mechanical properties of week 6 constructs increased relative to week 0 values ($p<0.05$, Fig. 6A). By week 8 (2 weeks after loading started), all samples had increased in modulus relative to preculture values, although no difference was detected between loaded and nonloaded constructs ($p=1.0$). However, an additional 2 weeks of cyclic conditioning induced a 16% increase in the tensile modulus of loaded samples compared to nonloaded controls ($p<0.001$). This increase in modulus was evident in average stress–strain plots of week 10 constructs, where loaded samples revealed a higher linear region slope than nonloaded controls (Fig. 6B).

While modulus is an intrinsic property of a material, changes in sample cross-sectional areas can preclude this measure from representing the actual changes in stiffness due to the production of load-bearing matrix. To eliminate any error introduced by alterations in cross-sectional area (observed in loaded constructs), gauge lengths were maintained identically across the entire study to enable the fair comparison of stiffness. Quantifying the percentage change relative to scaffold stiffness at week 0, the tensile contribution of newly synthesized ECM due to dynamic loading was isolated (Fig. 6C). While differences in stiffness were less exaggerated than those observed with tensile modulus, the identical trend was observed. After an initial increase in stiffness over the preculture period, 2 weeks of loading revealed no differences as a result of cyclic conditioning ($p=1.0$). However, with an additional 2 weeks of conditioning, loaded constructs continued to increase in stiffness ($p<0.001$ vs. week 8), whereas nonleaded controls plateaued at 8 week levels ($p=1.0$ vs. week 8).

Modulation of gene expression with dynamic loading

To better understand the molecular underpinnings of these biochemical and mechanical changes with tensile conditioning and dynamic culture, real-time reverse transcription-polymerase

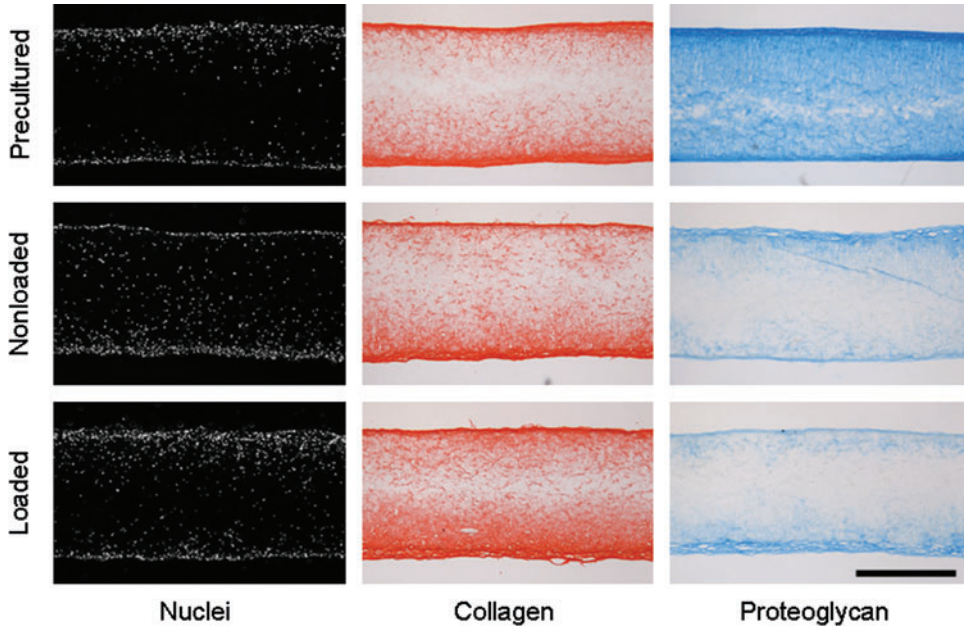

FIG. 5. Histological assessment of long-term dynamically loaded MSC constructs. Representative cross sections of precultured samples (week 6), and nonloaded controls and loaded constructs at week 10 stained with DAPI for cell nuclei, Picrosirius Red for collagens, and Alcian blue for proteoglycans (scale: 500 μm). Color images available online at www.liebertonline.com/tea

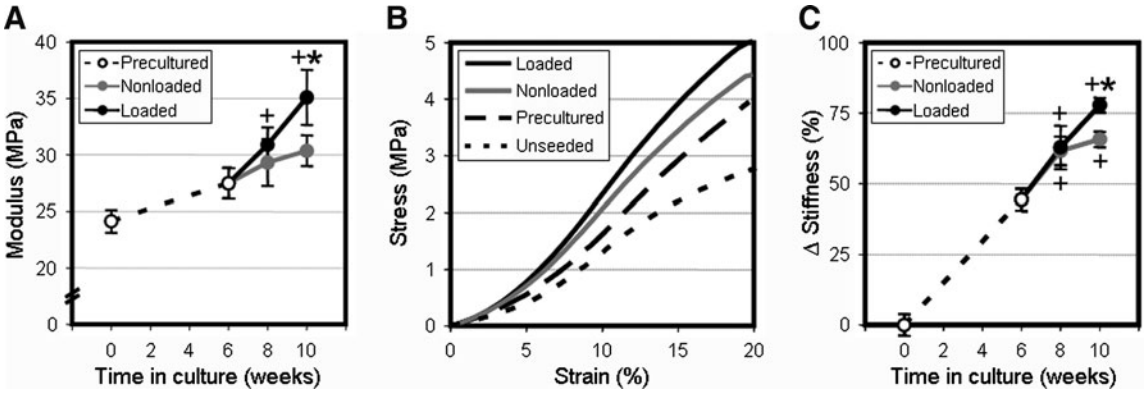

FIG. 6. Mechanical stimulation increases construct tensile properties. **(A)** Tensile modulus of precultured samples through week 6, and dynamically loaded constructs or nonloaded controls through week 10. **(B)** Average stress–strain curves of loaded and nonloaded constructs at the terminal time point, precultured samples at week 6, and acellular controls maintained in PBS for the duration of the study. **(C)** Change in stiffness normalized to initial (week 0) values ($n=6$, $^*p<0.05$ vs. nonloaded controls, $+p<0.05$ vs. precultured constructs).

chain reaction was performed on MSC-laden precultured constructs (week 6) and loaded/nonloaded constructs (week 10). Consistent with the increases in matrix content and tensile properties, cyclic loading had a pronounced effect on the expression of matrix and matrix-associated genes (Fig. 7). Four weeks of loading resulted in a two-fold increase in collagen I expression compared to nonloaded controls ($p<0.001$), with no effect on collagen II expression ($p=1.0$). Fibronectin, which is responsible for cell binding to the surrounding ECM and is a precursor to collagen deposition,[53] increased by two-fold with conditioning ($p<0.001$). Likewise, lysyl oxidase, an enzyme that cross-links collagen fibrils, was significantly upregulated in loaded constructs compared to nonloaded controls ($p<0.001$). Interestingly, compared to precultured samples, collagen II expression decreased markedly in both loaded and nonloaded samples ($p<0.001$, Fig. 7) and collagen I and fibronectin increased in nonloaded controls ($p<0.05$). Whether these changes were due to media agitation or are characteristic of the natural evolution of MSC-based nanofibrous constructs remains to be determined.

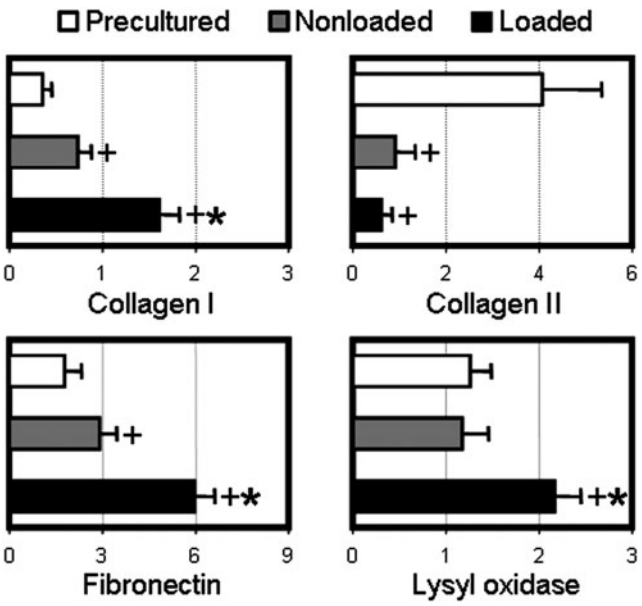

FIG. 7. Modulation of matrix-associated gene expression. Expression of collagen I, collagen II, fibronectin, and lysyl oxidase normalized to glyceraldehyde 3-phosphate dehydrogenase (GAPDH) expression levels for precultured samples (week 6) and loaded constructs or nonloaded controls at week 10 ($n=6$, $^*p<0.05$ vs. nonloaded controls, $+p<0.05$ vs. precultured constructs).

Discussion

With the goal of engineering *in vitro* tissues with biochemical and mechanical properties approximating native meniscal fibrocartilage, this study explored the effects of dynamic tensile stimulation on MSC-laden nanofibrous constructs. These constructs are founded on biocompatible and biodegradable scaffolds composed of aligned polymer nanofibers. The organization of nanofibers, which mimics the architecture of fibrous tissues such as the meniscus, dictates cell alignment and the organization of cell-deposited ECM.[21] In previous studies, the deposition of anisotropic fibrocartilaginous matrix under free-swelling, static culture conditions lead to demonstrable increases in the tensile properties of aligned nanofibrous constructs. However, even with long-term culture, the mechanical properties of constructs failed to achieve parity with native meniscus. Based upon abundant evidence that mechanical forces are necessary for the development and maintenance of load-bearing tissues, this study explored the effect of cyclic tension, the predominant loading modality of the meniscus, on the maturation of engineered constructs. With dynamic tensile stimulation that approximates the strains seen by meniscal fibrocartilage *in vivo*, we observed upregulation of fibrous gene expression and increases in the production of collagen, and demonstrated, for the first time, increases in the functional properties of tissue-engineered nanofibrous constructs.

In this work, we employed MSCs, a multipotent and readily available cell source that can be expanded *in vitro* for construct formation and can be induced to undergo fibrochondrogenic differentiation. MSC activity and fate decisions are sensitive to the cues they receive from their

surrounding microenvironment, which may arise from soluble or matrix-bound signaling molecules,[54] topographical features that inform cell shape and cytoskeletal organization,[55] passive mechanics such as matrix elasticity,[56] as well as active mechanical inputs[57,58] (for review, see Refs.[30,31]). In this study, the microenvironment is both complex and dynamic, as MSCs respond to and modulate their surroundings over the course of culture. MSC-laden nanofibrous constructs were cultured in the presence of TGF-β3, which promotes matrix synthesis[59] and can modulate MSC phenotype.[60] Beyond soluble factors, a topography of aligned nanofibers drives MSCs to adopt an elongated cell morphology with prominent actin stress fibers oriented in the direction of nanofiber alignment.[32] Coincident with these changes in shape, MSCs reduce chondrogenic markers, and upregulate fibrous gene expression compared to traditional pellet cultures. In addition to these passive cues, MSCs are highly sensitive to external mechanical perturbations, which can modulate phenotype depending on the modality of loading (i.e., compression vs. tension),[31] as well as the direction of loading with respect to the orientation of the cell.[61] Connelly and coworkers dynamically loaded MSCs within fibrin gels in tension and observed increases in type I collagen gene expression and protein production and no changes in traditional chondrogenic markers such as collagen II or aggrecan transcription or proteoglycan synthesis.[46] Paralleling these results, MSCs in this study responded to dynamic tensile stimulation with an increase in the expression of type I collagen, fibronectin (a precursor to collagen production[53]), and lysyl oxidase (a collagen fibril stabilizer and cross-linker) (Fig. 7), with no difference in collagen II expression or proteoglycan synthesis. These observations, combined with studies showing upregulation of chondrogenic factors under dynamic compression,[43–45] provide further evidence that MSCs will respond differently in terms of matrix biosynthesis depending on the loading modality to which they are exposed.

While MSC phenotype and alterations in gene expression are important considerations, the functional performance of ECM-rich, load-bearing engineered tissues arises from a complex cascade of protein translation, post-translational modifications, extracellular secretion and assembly, incorporation into the biomaterial scaffolding, and finally higher-order assembly and stabilization (e.g., collagen fibrillogenesis and cross-linking). Concurrent with the upregulation of collagen I gene expression, we observed increases in the production and incorporation of collagen with dynamic tensile loading (Fig. 4). These increases in total collagen content contributed to improvements in the tensile properties of nanofibrous constructs at week 10 (Fig. 6). Importantly, these increases occurred despite decreases in stiffness (6%) and modulus (13%) observed in acellular scaffolds exposed to the same loading regimen. Although the increase in stiffness can be partially accounted for by the increased collagen content,[62] dynamic loading also upregulated the expression of lysyl oxidase, which serves to cross-link and stabilize collagen networks. The degree of collagen fibril assembly that occurs within aligned nanofibrous scaffolds, and the activity of matrix-modifiers such as lysyl oxidase, both likely contribute to the resultant mechanical properties of tissue engineered constructs, and as such, are current subjects of investigation. Understanding the effect of mechanical forces at both the cellular (phenotype and biosynthetic activity) and tissue (matrix assembly, modification, and remodeling) levels in the context of an engineered construct may provide insights into how development proceeds in normal or diseased states, and will ultimately allow us to engineer tissues that better approximate the hierarchy, organization, and functional properties of native tissues.

The bioreactor employed in this study was designed with several features to enable ease of operation. Specifically, the modular design enabled simultaneous loading of multiple samples and straightforward insertion and removal of experimental groups. However, this design required the placement of constructs in fixtures in close proximity, presenting limitations in media diffusion under static culture conditions.[63] To maintain such arrayed constructs for the 4-week loading period while providing nutrient/waste transfer to centrally located constructs, dynamic culture conditions were employed during periods of rest. Perpetual agitation of the culture medium triggered a marked loss in GAG content (Figs. 4 and 5), an ECM component crucial to tissue compressive properties. Further, the depletion of GAGs may have impacted MSC gene expression, as collagen II expression decreased markedly in both loaded and nonloaded samples (Fig. 7). As meniscal fibrocartilage experiences both tensile and compressive forces at the same time, the removal of GAG from the ECM should be considered. Nerurkar *et al.* investigated the use of dynamic culture conditions toward enhancing cell infiltration and observed an identical loss of GAGs to the culture medium.[64] However, within 2 weeks of returning constructs to static conditions, GAGs were restored to levels on par with controls cultured statically for the duration of the study, suggesting the ready capacity of MSCs to synthesize this key matrix component.

While the positive changes in mechanical properties elicited by dynamic loading are encouraging (Fig. 6), the improvement in tensile modulus was 16% (compared to nonloaded controls), only slightly narrowing the gap between engineered fibrocartilage (35 MPa) and native meniscus tissue that possesses a fiber direction modulus between 65–80 MPa.[13] That being said, this study explored only one possible loading regimen (6%, 1 Hz, 3 h/day). It is plausible that a different combination of peak strain, frequency, and duty cycle applied over a longer duration would elicit a more dramatic cellular response and subsequent tissue maturation. In this work, 6% strain was chosen based on the deformations seen in the circumferential direction of the meniscus,[14,15] a value that is not necessarily optimized for MSCs on these scaffolds or at their current differentiation state. More recent studies in the meniscus have demonstrated that relative to macroscale tissue deformations, the microscale strains experienced by resident cells is highly varied and dependent upon the location of the cell relative to collagen fiber bundles and interstitial matrix.[65] Recently, we have begun to investigate how macroscale scaffold deformations translate to cellular and subcellular changes in MSCs on nanofibrous topographies.[66] While these studies were limited to surface-seeded cells, future studies employing such a macro-to-microscale approach to investigate MSC deformations in three-dimensional constructs will provide insights on how strain is transduced at the cellular level. Provided an understanding of this relationship, a systematic parameterization of loading regimens could then be explored

to identify the strain levels and frequencies that best drive ECM biosynthesis and assembly by resident MSCs.

An additional parameter that may play a role in determining how MSCs respond to tensile loading is the duration of preculture. In this study, 6 weeks of preculture was selected as it was a duration sufficient for cell colonization and elaboration of a functional, load-bearing ECM. MSCs will likely respond differently to external forces depending on the amount and character of their surrounding matrix. These differences could arise from the evolving mechanical properties of the surrounding matrix, which would dictate how loads are transferred through the ECM and to constituent cells. Alternatively, the presence and quantity of specific matrix components modulates cell–matrix adhesions, and this in turn will likely regulate mechanotransduction.[67] For example, Huang *et al.* found that MSCs responded favorably to dynamic compression in a three-dimensional hydrogel only after chondrogenesis had occurred.[57] Thus, the ideal preculture period and phenotypic status of the cells at the onset of loading requires further investigation.

Beyond demonstrating the potential for improving tissue construct maturation with mechanical stimulation, results from this study may have implications outside the realm of engineering *in vitro* tissues. In the case of implantation of an acellular scaffold into a load-bearing site, questions regarding patient rehabilitation arise. The improvements in construct development observed with mechanical stimulation in this study imply that as host cells colonize the implant, the dynamic tensile loading experienced with physiologic motion may have a beneficial effect in accelerating tissue regeneration and restoring mechanical function to the tissue. Indeed, the minimal loss in mechanical properties with repetitive loading suggests that the scaffolds are sufficiently robust to bear load when situated in a meniscal defect. On a more fundamental level, dynamic loading of aligned nanofibrous constructs can serve as model system for understanding how three-dimensional tissues composed of aligned arrays of cells embedded within organized ECM respond to mechanical stimuli and modulate their extracellular environment. Such a system provides a more controlled and experimentally compliant approach to studying mechanotransduction, as compared to studies performed with native tissues that are susceptible to donor variability and intratissue regionality. Future studies using this system will provide insights into the intricate interplay between cells, the extracellular microenvironment, and mechanical perturbations. Coming full circle, elucidation of the signaling mechanisms underlying the biosynthetic response of MSCs to mechanical inputs could then be applied in identifying the timing and parameters of an optimized loading regimen for improving the *in vitro* maturation of engineered tissues for meniscus and other fibrous tissue repair.

Acknowledgments

This work was supported by the National Institutes of Health (R01 AR056624) and an Orthopaedic Medicine Research Grant from the Aircast Foundation (F0206R). Additional support was provided by the Penn Center for Musculoskeletal Disorders and a National Science Foundation Graduate Research Fellowship (B.M.B.). A preliminary version of this work was published as part of a doctoral dissertation (B.M.B.) and is publicly available through the University of Pennsylvania Library.[68]

Disclosure Statement

No competing financial interests exist.

References

1. Messner, K., and Gao, J. The menisci of the knee joint. Anatomical and functional characteristics, and a rationale for clinical treatment. J Anat **193 (Pt 2),** 161, 1998.
2. Greis, P.E., Bardana, D.D., Holmstrom, M.C., and Burks, R.T. Meniscal injury: I. Basic science and evaluation. J Am Acad Orthop Surg **10,** 168, 2002.
3. Shrive, N.G., O'Connor, J.J., and Goodfellow, J.W. Load-bearing in the knee joint. Clin Orthop **131,** 279, 1978.
4. Setton, L.A., Guilak, F., Hsu, E.W., and Vail, T.P. Biomechanical factors in tissue engineered meniscal repair. Clin Orthop **367 Suppl,** S254, 1999.
5. Fithian, D.C., Kelly, M.A., and Mow, V.C. Material properties and structure-function relationships in the menisci. Clin Orthop **252,** 19, 1990.
6. Petersen, W., and Tillmann, B. Collagenous fibril texture of the human knee joint menisci. Anat Embryol (Berl) **197,** 317, 1998.
7. McDevitt, C.A., and Webber, R.J. The ultrastructure and biochemistry of meniscal cartilage. Clin Orthop Relat Res **252,** 8, 1990.
8. Eyre, D.R., and Wu, J.J. Collagen of fibrocartilage: a distinctive molecular phenotype in bovine meniscus. FEBS Lett **158,** 265, 1983.
9. Adams, M.E., and Hukins, D.W.L. The extracellular matrix of the meniscus. In: Mow, V.C., Arnoczky, S.P., Jackson, D.W., eds. Knee Meniscus: Basic and Clinical Foundations. New York: Raven Press, Ltd., 1992, pp. 15–28.
10. O'Connor, B.L. The histological structure of dog knee menisci with comments on its possible significance. Am J Anat **147,** 407, 1976.
11. Seedhom, B.B. Loadbearing function of the menisci. Physiotherapy **62,** 223, 1976.
12. Ahmed, A.M., and Burke, D.L. *In-vitro* measurement of static pressure distribution in synovial joints—Part I: tibial surface of the knee. J Biomech Eng **105,** 216, 1983.
13. Bursac, P., York, A., Kuznia, P., Brown, L.M., and Arnoczky, S.P. Influence of donor age on the biomechanical and biochemical properties of human meniscal allografts. Am J Sports Med **37,** 884, 2009.
14. Jones, R.S., Keene, G.C., Learmonth, D.J., Bickerstaff, D., Nawana, N.S., Costi, J.J., *et al.* Direct measurement of hoop strains in the intact and torn human medial meniscus. Clin Biomech (Bristol, Avon) **11,** 295, 1996.
15. Richards, C.J., Gatt, C.J., Langrana, N., and Calderon, R. Quantitative measurement of human meniscal strain. Trans Orthop Res Soc **28,** 649, 2003.
16. MacAusland, W.R. Derangements of the semilunar cartilages. Ann Surg **93,** 649, 1931.
17. Cravener, E.K., and MacElroy, D.G. Injuries of the internal semilunar cartilage. JAMA **117,** 1695, 1941.
18. Rath, E., and Richmond, J.C. The menisci: basic science and advances in treatment. Br J Sports Med **34,** 252, 2000.
19. Englund, M., Roos, E.M., and Lohmander, L.S. Impact of type of meniscal tear on radiographic and symptomatic knee osteoarthritis: a sixteen-year followup of meniscectomy with matched controls. Arthritis Rheum **48,** 2178, 2003.

20. Meredith, D.S., Losina, E., Mahomed, N.N., Wright, J., and Katz, J.N. Factors predicting functional and radiographic outcomes after arthroscopic partial meniscectomy: a review of the literature. Arthroscopy **21,** 211, 2005.
21. Baker, B.M., and Mauck, R.L. The effect of nanofiber alignment on the maturation of engineered meniscus constructs. Biomaterials **28,** 1967, 2007.
22. Deitzel, J.M., Kleinmeyer, J., Harris, D., and Beck Tan, N.C. The effect of processing variables on the morphology of electrospun nanofibers and textiles. Polymer **42,** 261, 2001.
23. Li, W.J., Mauck, R.L., Cooper, J.A., Yuan, X., and Tuan, R.S. Engineering controllable anisotropy in electrospun biodegradable nanofibrous scaffolds for musculoskeletal tissue engineering. J Biomech **40,** 1686, 2007.
24. Ayres, C., Bowlin, G.L., Henderson, S.C., Taylor, L., Shultz, J., Alexander, J., *et al.* Modulation of anisotropy in electrospun tissue-engineering scaffolds: analysis of fiber alignment by the fast Fourier transform. Biomaterials **27,** 5524, 2006.
25. Courtney, T., Sacks, M.S., Stankus, J., Guan, J., and Wagner, W.R. Design and analysis of tissue engineering scaffolds that mimic soft tissue mechanical anisotropy. Biomaterials **27,** 3631, 2006.
26. Mauck, R.L., Baker, B.M., Nerurkar, N.L., Burdick, J.A., Li, W.J., Tuan, R.S., *et al.* Engineering on the straight and narrow: the mechanics of nanofibrous assemblies for fiber-reinforced tissue regeneration. Tissue Eng Part B Rev **15,** 171, 2009.
27. Caplan, A.I. Mesenchymal stem cells. J Orthop Res **9,** 641, 1991.
28. Caplan, A.I. Review: mesenchymal stem cells: cell-based reconstructive therapy in orthopedics. Tissue Eng **11,** 1198, 2005.
29. Nerurkar, N.L., Baker, B.M., Sen, S., Wible, E.E., Elliott, D.M., and Mauck, R.L. Nanofibrous biologic laminates replicate the form and function of the annulus fibrosus. Nat Mater **8,** 986, 2009.
30. Discher, D.E., Mooney, D.J., and Zandstra, P.W. Growth factors, matrices, and forces combine and control stem cells. Science **324,** 1673, 2009.
31. Guilak, F., Cohen, D.M., Estes, B.T., Gimble, J.M., Liedtke, W., and Chen, C.S. Control of stem cell fate by physical interactions with the extracellular matrix. Cell Stem Cell **5,** 17, 2009.
32. Baker, B.M., Nathan, A.S., Gee, A.O., and Mauck, R.L. The influence of an aligned nanofibrous topography on human mesenchymal stem cell fibrochondrogenesis. Biomaterials **31,** 6190, 2010.
33. Baker, B.M., Silverstein, A.M., Shah, R.P., and Mauck, R.L. Matrix deposition modulates the dynamic mechanical behavior of nanofiber-based fibrocartilage. Trans Orthop Res Soc **35,** 1312. 2010.
34. Carter, D.R. Mechanical loading history and skeletal biology. J Biomech **20,** 1095, 1987.
35. Kardon, G. Muscle and tendon morphogenesis in the avian hind limb. Development **125,** 4019, 1998.
36. Kahn, J., Shwartz, Y., Blitz, E., Krief, S., Sharir, A., Breitel, D.A., *et al.* Muscle contraction is necessary to maintain joint progenitor cell fate. Dev Cell **16,** 734, 2009.
37. Mikic, B., Johnson, T.L., Chhabra, A.B., Schalet, B.J., Wong, M., and Hunziker, E.B. Differential effects of embryonic immobilization on the development of fibrocartilaginous skeletal elements. J Rehabil Res Dev **37,** 127, 2000.
38. Butler, D.L., Goldstein, S.A., and Guilak, F. Functional tissue engineering: the role of biomechanics. J Biomech Eng **122,** 570, 2000.
39. Mauck, R.L., Soltz, M.A., Wang, C.C., Wong, D.D., Chao, P.H., Valhmu, W.B., *et al.* Functional tissue engineering of articular cartilage through dynamic loading of chondrocyte-seeded agarose gels. J Biomech Eng **122,** 252, 2000.
40. Garvin, J., Qi, J., Maloney, M., and Banes, A.J. Novel system for engineering bioartificial tendons and application of mechanical load. Tissue Eng **9,** 967, 2003.
41. Juncosa-Melvin, N., Shearn, J.T., Boivin, G.P., Gooch, C., Galloway, M.T., West, J.R., *et al.* Effects of mechanical stimulation on the biomechanics and histology of stem cell-collagen sponge constructs for rabbit patellar tendon repair. Tissue Eng **12,** 2291, 2006.
42. Lee, C.H., Shin, H.J., Cho, I.H., Kang, Y.M., Kim, I.A., Park, K.D., *et al.* Nanofiber alignment and direction of mechanical strain affect the ECM production of human ACL fibroblast. Biomaterials **26,** 1261, 2005.
43. Huang, C.Y., Reuben, P.M., D'Ippolito, G., Schiller, P.C., and Cheung, H.S. Chondrogenesis of human bone marrow-derived mesenchymal stem cells in agarose culture. Anat Rec A Discov Mol Cell Evol Biol **278,** 428, 2004.
44. Mouw, J.K., Connelly, J.T., Wilson, C.G., Michael, K.E., and Levenston, M.E. Dynamic compression regulates the expression and synthesis of chondrocyte-specific matrix molecules in bone marrow stromal cells. Stem Cells **25,** 655, 2007.
45. Mauck, R.L., Byers, B.A., Yuan, X., and Tuan, R.S. Regulation of cartilaginous ECM gene transcription by chondrocytes and MSCs in 3D culture in response to dynamic loading. Biomech Model Mechanobiol **6,** 113, 2007.
46. Connelly, J.T., Vanderploeg, E.J., Mouw, J.K., Wilson, C.G., and Levenston, M.E. Tensile loading modulates bone marrow stromal cell differentiation and the development of engineered fibrocartilage constructs. Tissue Eng Part A **16,** 1913, 2010.
47. Mauck, R.L., Yuan, X., and Tuan, R.S. Chondrogenic differentiation and functional maturation of bovine mesenchymal stem cells in long-term agarose culture. Osteoarthritis Cartilage **14,** 179, 2006.
48. Peltz, C.D., Perry, S.M., Getz, C.L., and Soslowsky, L.J. Mechanical properties of the long-head of the biceps tendon are altered in the presence of rotator cuff tears in a rat model. J Orthop Res **27,** 416, 2009.
49. Farndale, R.W., Buttle, D.J., and Barrett, A.J. Improved quantitation and discrimination of sulphated glycosaminoglycans by use of dimethylmethylene blue. Biochim Biophys Acta **883,** 173, 1986.
50. Stegemann, H., and Stalder, K. Determination of hydroxyproline. Clin Chim Acta **18,** 267, 1967.
51. Neuman, R.E., and Logan, M.A. The determination of hydroxyproline. J Biol Chem **184,** 299, 1950.
52. Huang, A.H., Stein, A., Tuan, R.S., and Mauck, R.L. Transient exposure to transforming growth factor beta 3 improves the mechanical properties of mesenchymal stem cell-laden cartilage constructs in a density-dependent manner. Tissue Eng Part A **15,** 3461, 2009.
53. Li, S., Van Den Diepstraten, C., D'Souza, S.J., Chan, B.M., and Pickering, J.G. Vascular smooth muscle cells orchestrate the assembly of type I collagen via alpha2beta1 integrin, RhoA, and fibronectin polymerization. Am J Pathol **163,** 1045, 2003.
54. Pittenger, M.F., Mackay, A.M., Beck, S.C., Jaiswal, R.K., Douglas, R., Mosca, J.D., *et al.* Multilineage potential of adult human mesenchymal stem cells. Science **284,** 143, 1999.

55. McBeath, R., Pirone, D.M., Nelson, C.M., Bhadriraju, K., and Chen, C.S. Cell shape, cytoskeletal tension, and RhoA regulate stem cell lineage commitment. Dev Cell **6,** 483, 2004.
56. Engler, A.J., Sen, S., Sweeney, H.L., and Discher, D.E. Matrix elasticity directs stem cell lineage specification. Cell **126,** 677, 2006.
57. Huang, A.H., Farrell, M.J., Kim, M., and Mauck, R.L. Long-term dynamic loading improves the mechanical properties of chondrogenic mesenchymal stem cell-laden hydrogel. Eur Cell Mater **19,** 72, 2010.
58. Simmons, C.A., Matlis, S., Thornton, D.J., Chen, S., Wang, C.Y., and Mooney, D.J. Cyclic strain enhances matrix mineralization by adult human mesenchymal stem cells via the extracellular signal-regulated kinase (ERK1/2) signaling pathway. J Biomech **36,** 1087, 2003.
59. Li, W.J., Tuli, R., Huang, X., Laquerriere, P., and Tuan, R.S. Multilineage differentiation of human mesenchymal stem cells in a three-dimensional nanofibrous scaffold. Biomaterials **26,** 5158, 2005.
60. Gao, L., McBeath, R., and Chen, C.S. Stem cell shape regulates a chondrogenic versus myogenic fate through Rac1 and N-cadherin. Stem Cells **28,** 564, 2010.
61. Kurpinski, K., Chu, J., Hashi, C., and Li, S. Anisotropic mechanosensing by mesenchymal stem cells. Proc Natl Acad Sci U S A **103,** 16095, 2006.
62. Baker, B.M., Nathan, A.S., Huffman, G.R., and Mauck, R.L. Tissue engineering with meniscus cells derived from surgical debris. Osteoarthritis Cartilage **17,** 336, 2009.
63. Baker, B.M., Silverstein, A.M., and Mauck, R.L. Engineering dense connective tissues via anisotropic nanofibrous scaffolds with high sacrificial fiber content. Proc ASME 2010 First Global Congress on NanoEngineering for Medicine and Biology 13371, 2010.
64. Nerurkar, N.L., Sen, S., Baker, B.M., Elliott, D.M., and Mauck, R.L. Dynamic culture enhances stem cell infiltration and modulates extracellular matrix production on aligned electrospun nanofibrous scaffolds. Acta Biomater **7,** 485, 2011.
65. Upton, M.L., Gilchrist, C.L., Guilak, F., and Setton, L.A. Transfer of macroscale tissue strain to microscale cell regions in the deformed meniscus. Biophys J **95,** 2116, 2008.
66. Nathan, A.S., Baker, B.M., Nerurkar, N.L., and Mauck, R.L. Mechano-topographic modulation of stem cell nuclear shape on nanofibrous scaffolds. Acta Biomater **7,** 57, 2011.
67. Chen, C.S., Tan, J., and Tien, J. Mechanotransduction at cell-matrix and cell-cell contacts. Annu Rev Biomed Eng **6,** 275, 2004.
68. Baker, B.M. Meniscus Tissue Engineering with Nanofibrous Scaffolds [Ph.D. Dissertation]. Department of Bioengineering, University of Pennsylvania, Philadelphia, PA, 2010 (http://repository.upenn.edu/edissertations/212/).

Address correspondence to:
Robert L. Mauck, Ph.D.
McKay Orthopaedic Research Laboratory
Department of Orthopaedic Surgery
University of Pennsylvania
424G Stemmler Hall
36th St. and Hamilton Walk
Philadelphia, PA 19104

E-mail: lemauck@mail.med.upenn.edu

Received: September 8, 2010
Accepted: January 18, 2011
Online Publication Date: March 1, 2011